ELSEVIER

Chemical Geology 221 (2005) 170–187

CHEMICAL GEOLOGY
INCLUDING
ISOTOPE GEOSCIENCE

www.elsevier.com/locate/chemgeo

Zn and Cu isotopic variability in the Alexandrinka volcanic-hosted massive sulphide (VHMS) ore deposit, Urals, Russia

Thomas F.D. Mason[a], Dominik J. Weiss[a,b,*], John B. Chapman[a,b], Jamie J. Wilkinson[a,b], Svetlana G. Tessalina[c], Baruch Spiro[b], Matthew S.A. Horstwood[d], John Spratt[b], Barry J. Coles[a,b]

[a]*Department of Earth Science and Engineering, Imperial College London, Exhibition Road, London, SW7 2AZ, UK*
[b]*Department of Mineralogy, Natural History Museum, Cromwell Road, London, SW7 5BD, UK*
[c]*Laboratoire de Géochimie et Cosmochimie, Institute de Physique du Globe, 75252 Paris Cédex 05, France*
[d]*NERC Isotope Geosciences Laboratory, Kingsley Dunham Centre, Keyworth, Nottingham, NG12 5GG, UK*

Received 2 September 2004; received in revised form 31 March 2005; accepted 24 April 2005

Abstract

Copper and Zn isotope ratios of well-characterized samples from three ore facies in the Devonian Alexandrinka volcanic-hosted massive sulphide (VHMS) deposit, southern Urals, were measured using multi collector ICP-MS (MC-ICP-MS) and show variations linked to depositional environment and mineralogy. The samples analysed derived from: a) hydrothermal–metasomatic vein stockwork, b) a hydrothermal vent chimney, and c) reworked clastic sulphides. As the deposit has not been significantly deformed or metamorphosed after its formation, it represents a pristine example of ancient seafloor mineralization. Variations in $\delta^{65}Cu$ (where $\delta^{65}Cu=[(^{65}Cu/^{63}Cu)_{sample}/(^{65}Cu/^{63}Cu)_{standard}-1]*1000$) and $\delta^{66}Zn$ (where $\delta^{66}Zn=[(^{66}Zn/^{64}Zn)_{sample}/(^{66}Zn/^{64}Zn)_{standard}-1]*1000$) of 0.63 and 0.66‰, respectively, are significantly greater than analytical uncertainty for both isotope ratios (± 0.07‰, 2σ). Very limited isotopic fractionation is observed in primary Cu minerals from the stockwork and chimney, whereas the Zn isotopic composition of the stockwork varies significantly with the mineralogy. Chalcopyrite-bearing samples from the stockwork have lighter $\delta^{66}Zn$ by ~0.4‰ relative to sphalerite dominated samples, which may be due to equilibrium partitioning of isotopically light Zn into chalcopyrite during its precipitation. $\delta^{66}Zn$ also showed significant variation in the chimney, with an enrichment in heavy isotopes toward the chimney rim of ~0.26‰, which may be caused by changing temperature (hence fractionation factor), or Raleigh distillation. Post-depositional seafloor oxidative dissolution and re-precipitation in the clastic sediments, possibly coupled with leaching, led to systematic negative shifts in Cu and Zn isotope compositions relative to the primary sulphides. Copper shows the most pronounced fractionation, consistent with the reduction of Cu(II) to Cu(I) during supergene mineralization. However, the restricted range in $\delta^{65}Cu$ is unlike modern sulphides at mid oceanic ridges where a large range of Cu isotope, of up to 3‰ has been observed [Rouxel, O., Fouquet, Y., Ludden, J.N., 2004. Copper isotope systematics of the Lucky Strike, Rainbow, and Logatchev sea-floor hydrothermal fields on

* Corresponding author. Department of Earth Science and Engineering, Imperial College London, Exhibition Road, London, SW7 2AZ, UK. Fax: +44 20 7594 7444.
E-mail address: d.weiss@imperial.ac.uk (D.J. Weiss).

0009-2541/$ - see front matter
doi:10.1016/j.chemgeo.2005.04.011

the Mid-Atlantic Ridge. Econ. Geol. 99, 585–600; Zhu, X.K., O'Nions, R.K., Guo, Y., Belshaw, N.S., Rickard, D., 2000. Determination of natural Cu-isotope variation by plasma source mass spectrometry: implications for use as geochemical tracers. Chem. Geol. 163, 139–149].

Keywords: MC-ICP-MS; VHMS deposits; Seafloor hydrothermal vent system; Isotope fractionation; Copper isotopes; Zinc isotopes

1. Introduction

Since the advent of multiple collector inductively-coupled plasma mass spectrometry (MC-ICP-MS) it has become possible to study the isotope geochemistry of transition metals in natural systems. Precisions for Cu and Zn ratios are typically ± 0.1‰ (2σ) or better for both Zn/Cu doping and sample standard bracketing techniques (Mason et al., 2004a,b). This has led to the discovery of significant isotope fractionation of these elements caused by various geochemical and biogeochemical processes (Johnson et al., 2004; Larson et al., 2003; Rouxel et al., 2004; Weiss et al., 2005; Zhu et al., 2002, 2000).

Owing to elevated metal contents and well-constrained formation conditions, ore deposits are particularly suitable for studies of isotope fractionation. Consequently, a number of preliminary investigations of hydrothermal and magmatic ore forming environments (marine and terrestrial alike) have been conducted and possible controlling mechanisms have been proposed. Most of this work has concentrated on Cu (Blix et al., 1957; Gale et al., 1999; Graham et al., 2004; Jiang et al., 2002; Larson et al., 2003; Maréchal et al., 1999; Rouxel et al., 2004; Shields et al., 1965; Zhu et al., 2000), which is expected to show more significant isotope variations due to the importance of redox-reactions, with very little information on the behaviour of Zn (Wilkinson et al., in press).

Published δ^{65}Cu data for primary Cu-rich minerals from terrestrial and marine hydrothermal deposits display a relatively narrow range from −1.06 to 1.41‰ with a mean value of 0.03‰ (relative to NIST-SRM 976 Cu) (Gale et al., 1999; Graham et al., 2004; Larson et al., 2003; Maréchal et al., 1999; Shields et al., 1965; Walker et al., 1958; Zhu et al., 2000). By contrast, supergene Cu minerals that formed during oxidation and weathering of primary sulphide ores yield a wide range of δ^{65}Cu values (from −8.4 to 9.1‰, including early TIMS data), with a general shift towards isotopically heavy compositions compared with inferred precursor minerals. For example, native Cu from the Michigan District (USA) defines a relatively narrow range of Cu isotopic compositions of c. 0.1‰ compared to secondary Cu-sulphides and arsenides from the same deposits that yield a range of c. 2‰ (Larson et al., 2003). Large isotopic variations for Cu have also been reported in a sediment-hosted hydrothermal vein-type deposit from Jinman, China (Jiang et al., 2002), with a range in δ^{65}Cu of −3.70 to 0.30‰. The most negative δ^{65}Cu values were from chalcopyrite precipitated at lower temperatures (c. 150 °C), while the most positive value represented a chalcopyrite from a high-temperature feeder vein (c. 286 °C), linking δ^{65}Cu to formation temperature. Graham et al. (2004) conducted the only study on igneous intrusions to date, using three intrusions that make up the Grasberg Igneous Complex. δ^{65}Cu showed a limited range from 0.02 to 1.34‰ and two dominant processes were put forward to explain the observed variation: (i) isotope fractionation during distillation from the underlying source and establishment of hydrothermal cells associated with each intrusion and (ii) isotope fractionation as the ore bearing fluid moved outward from a central core (Graham et al., 2004).

Copper isotope data from modern submarine hydrothermal vent systems support the link between shifts in δ^{65}Cu and secondary, low-temperature processes (Rouxel et al., 2004; Zhu et al., 2000). Chalcopyrite separates from active hydrothermal chimneys from the East Pacific Rise, Galapagos Ridge, and Broken Spur hydrothermal fields, yielded positive δ^{65}Cu values from 0.31 to 1.16‰, while inactive chimneys from the same sites were systematically lighter, with δ^{65}Cu values between −0.48 and −0.19‰ (Zhu et al., 2000). These variations possibly reflect selective leaching of ^{65}Cu from the source

rock, imparting an isotopically heavy signature to the growing active vents. In a more recent and detailed study, Rouxel et al. (2004) presented Cu isotope signatures from black smoker sulphides, massive sulphides and their alteration products from three hydrothermal fields on the Mid-Atlantic Ridge: Lucky Strike, Rainbow, and Logatchev. Precipitation of Cu rich sulphides seemed to have had only a small effect on the δ^{65}Cu values, compared to the subsequent alteration which resulted in a shift in δ^{65}Cu of up to 3‰. Massive sulphides characterised by negative δ^{65}Cu have undergone extensive recrystallisation (Rouxel et al., 2004).

The isotopic behaviour of Zn in the ore-forming environment remains very poorly constrained. Significant variation of up to 0.75‰ pamu was reported in the Zn isotopic compositions of sphalerite separates from the carbonate-hosted Zn–Pb deposits of the Irish ore-field (Wilkinson et al., in press). This work suggested that source rock composition or temperature variations were unlikely to be important controls on the zinc isotope composition of sphalerite in the ore field. The authors inferred that the variation was most likely to be due to kinetic fractionation involving the preferential incorporation of light Zn isotopes into sphalerite precipitated rapidly under disequilibrium conditions. However, they could not rule out the possibility of mixing of zinc derived from two, isotopically distinct, sources. Significant isotopic variations for Zn have also been reported in microbially-mediated sulphide ores with δ^{66}Zn increasing by 0.8‰ in tandem with an increase in sulphur content of bacterial origin (Archer and Vance, 2002). In this study, the isotopic shifts in Zn mirrored a decrease in δ^{65}Cu of −0.9‰, suggesting the involvement of biological processes.

Given the limited data on the Zn and Cu isotopic composition of ore materials and the uncertainties in the controls of isotopic fractionation, we carried out an investigation of the isotopic variability of Cu and Zn in the Alexandrinka volcanic-hosted massive sulphide (VHMS) ore deposit. This study gained new insights into Cu and Zn isotope geochemistry in seafloor hydrothermal systems and increased the potential to exploit application of these new isotopic systems to the study of base metal deposits.

2. Geological background

The Alexandrinka VHMS ore deposit, formed during the Middle Devonian, has not been subjected to pronounced deformation or metamorphism, and thus represents a virtually pristine example of ancient seafloor mineralization (Herrington et al., 2002; Tessalina et al., 1999, 2001). The deposit contains Cu- and Zn-rich ores of both primary and secondary origin and provides an ideal opportunity to investigate the controls on the isotopic composition of Cu and Zn during moderately high-temperature hydrothermal processes (up to c. 310 °C) beneath and within submarine vent complexes, and during low-temperature seafloor weathering of reworked clastic sulphides.

2.1. Location and geological setting

The Alexandrinka deposit is situated at 52°01′N, 58°50′E, 25 km northeast of Magnitogorsk, in the southern Urals, Russia (Fig. 1). It is one of a series of VHMS ore bodies that are hosted in the remnants of the East-Magnitogorsk island arc (Belogub et al., 2003; Herrington et al., 2002; Prokin et al., 1998; Sigov, 1969; Tessalina et al., 1999, 2001). The ore body is notable for its relative elevated grades of base (4.4 wt.% Cu and 5.5 wt.% Zn) and precious metals (2.2 ppm Au and 57 ppm Ag), and has been classified as a Baimak- or Kuroko-type deposit (Prokin et al., 1998).

The deposit occurs at the contact between basalts and underlying rhyolites of the Karamalytsh Formation. The host rock comprises lavas and hyaloclastites of aphyric and fine-porphyritic dacites, with fragments of basalt, plagioclase–quartz rhyolite, aphyric andesite–dacite, secondary quartzite, jasper, and chloritised volcanic rocks. The ore body lies in a NE-trending, 10 km long, linear depression that is thought to reflect the original geometry of the paleo-hydrothermal field (Tessalina et al., 1999).

2.2. Mechanisms of ore formation

The Alexandrinka deposit represents the remnants of a collapsed hydrothermal vent complex (Tessalina et al., 2001). Towards the north of the ore unit, a degraded sulphide mound is preserved, from which fragments of hydrothermal vent chimneys have been

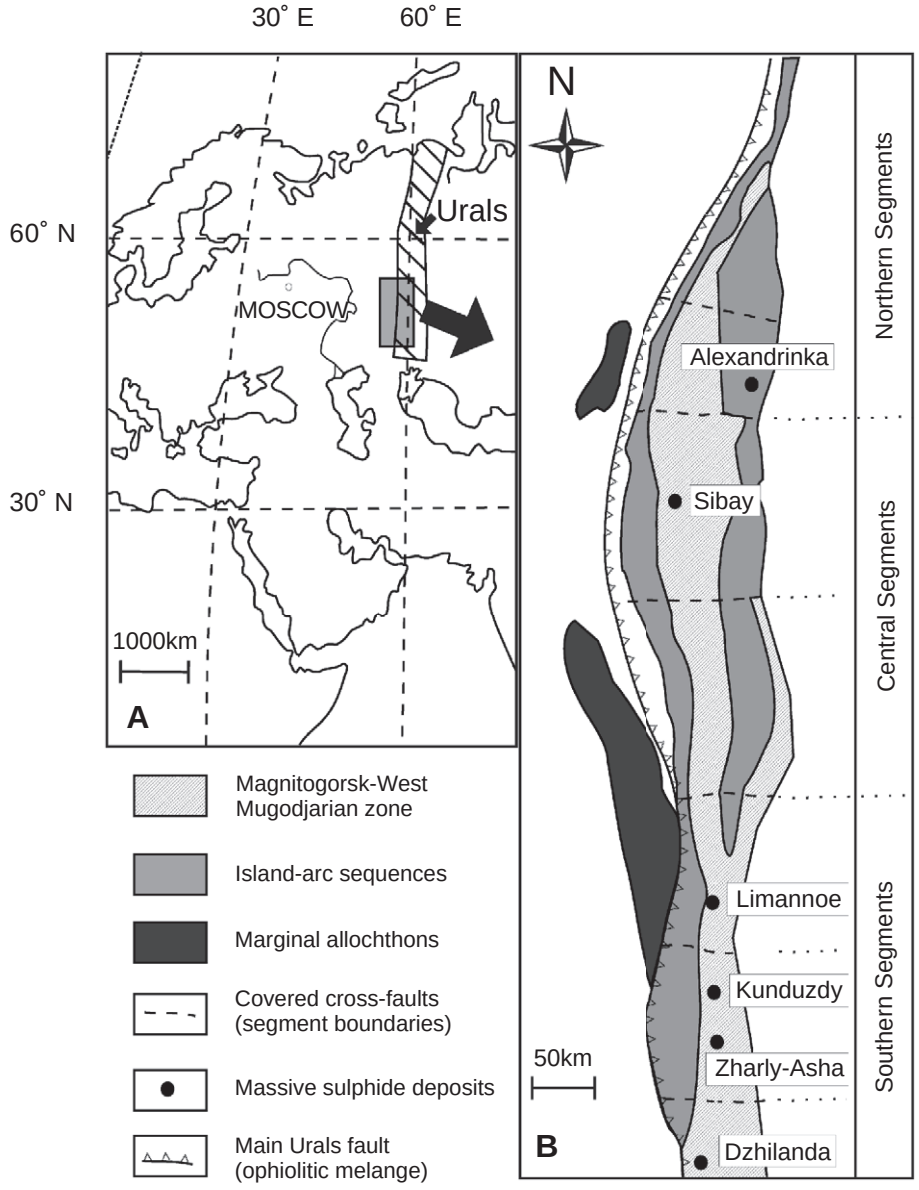

Fig. 1. Locality of the Alexandrinka volcanic hosted massive sulphide deposit (Southern Urals, Russia) within the Devonian paleo-oceanic structure.

recovered (Herrington et al., 2002). These share a similar mineral association, texture, and zonation to vent complexes currently forming on the ocean floor, e.g. the southern Juan de Fuca Ridge (Shanks and Seyfried, 1987), and to ancient hydrothermal chimneys at Kuroko (Scott, 1981), indicating a sea-floor exhalative origin. Drilling below the sulphide mound has revealed a stockwork of mineralised veins, interpreted as the feeder zone to the vent complex.

The majority of ore-grade material lies to the south of the sulphide mound. This orebody originated from the mechanical degradation of the hydrothermal vent complex and subsequent down-slope transport of sul-

phide clasts by turbidity flows. Such sedimentary processing is consistent with the observed lateral- and vertical-grading of sulphide clasts away from the sulphide mound (Tessalina et al., 1999).

Syn- and post-depositional remobilisation of precious and base metals has modified their distribution within the ore body (Tessalina et al., 1999, 2001). A series of 'paleo-surfaces', classified as seafloor gossans, occur within the ore sequence. These horizons have undergone extensive alteration to hematite, chlorite, illite–smectite clays, quartz, barite, and carbonates. There is evidence that the metals released during alteration were transported down-section through the sulphide sediments, before being partially reprecipitated at depth (Tessalina et al., 2001). This has led to a supergene assemblage of base-metal sulphides in the lower horizons of the deposit, with the formation of a variety of secondary ore minerals including covellite (CuS), chalcocite (Cu_2S), and bornite (Cu_5FeS_4), in addition to large quantities of secondary chalcopyrite and sphalerite.

Fig. 2 shows a schematic drawing of the possible structure of the hydrothermal vent system including the three dominant ore-grade facies (see below).

3. Methodology

3.1. Sample descriptions

The Alexandrinka deposit comprises three ore-grade facies (Tessalina et al., 1999): (1) a hydrothermal–metasomatic stockwork; (2) seafloor–hydrothermal chimneys; and (3) clastic sedimentary deposits. From these major zones, specimens were selected for investigation and samples were taken by microdrill. Samples represent both mineral separates and mixtures. Seafloor sulphides are in general complexly intergrown and typically very fine grained, therefore separation of pure mineral phases was very difficult to achieve, and virtually impossible for the secondary phases.

A hand specimen from a core drilled below the sulphide mound, was selected to represent the stockwork. Six samples (SW-1(a) to SW-1(f)) were drilled from a traverse perpendicular to the mineralogical banding, to provide a record of spatial and mineralogical variability through the specimen. The locations of these samples are shown in Fig. 3A.

A sample of sulphide chimney from the remnant sulphide mound was selected to represent the seafloor

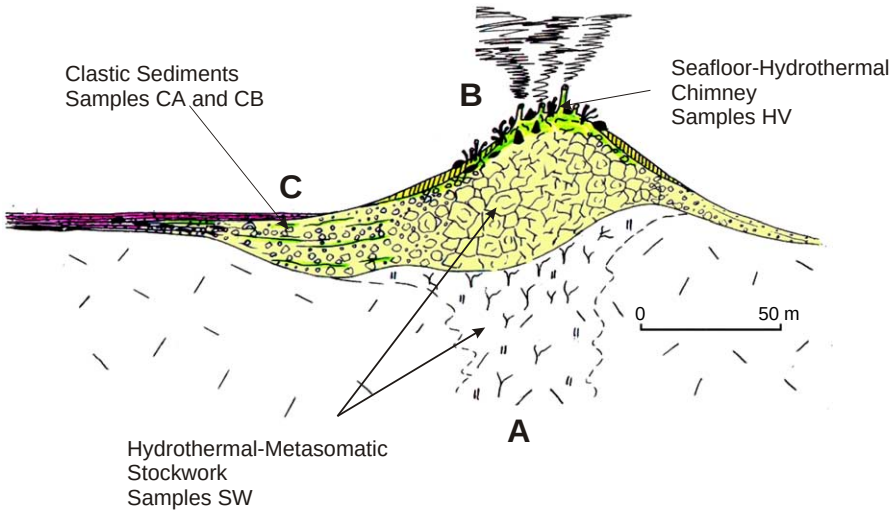

Fig. 2. Schematic representation of a hydrothermal vent system indicating the major facies seen at Alexandrinka: hydrothermal–metasomatic stockwork, seafloor–hydrothermal chimney, and clastic sediments. Three dominant processes were involved in ore genesis (Tessalina et al., 1999, 2001): (A) Metal-bearing fluids originating from depth migrated up to the seafloor, mineralising the basement rocks (stockwork, SW); (B) At the seafloor these fluids rapidly precipitated metal sulphides leading to the formation of a hydrothermal vent complex (chimney, HV); (C) The resultant sulphide mound was then degraded, and sulphide material was transported down-slope by turbidity currents to form sorted clastic sediment, and post-depositional alteration within the clastic sediments subsequently redistributed Cu and Zn down-section.

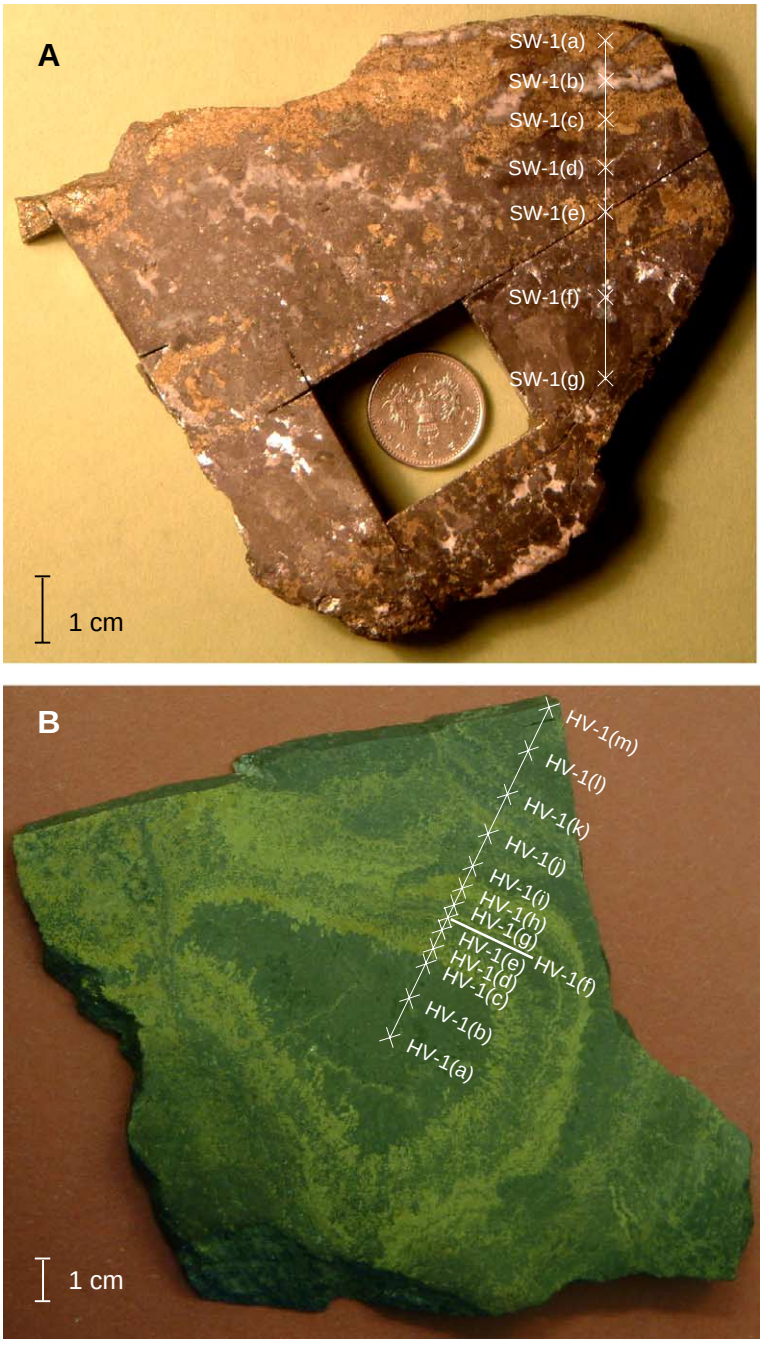

Fig. 3. Photographs of stockwork (a, SW-1) and hydrothermal chimney (b, HV-1) samples used for this study. Sub-sample transect lines and microdrilling locations are also shown. A) Stockwork sample showing pronounced mineral zonation. Zones comprise chalcopyrite + pyrite (brassy yellow), galena + minor chalcopyrite and sphalerite (pale grey), sphalerite + minor chalcopyrite and galena (dark grey), and quartz + barite gangue (white). Coin is 18 mm in diameter. B) Vent sample showing concentric mineral zonation. The sphalerite-dominated core (dark grey) is surrounded by bands with compositions dominated by chalcopyrite (brassy yellow) or sphalerite. At the outer edge (HV-1(k) to HV-1(m)) the sample is surrounded by a sphalerite-dominated carapace. (For interpretation of the references to colour in this figure legend, the reader is referred to the web version of this article.)

hydrothermal facies. This specimen provided a cross-section through the preserved chimney structure. Thirteen samples (HV-1(a) to HV-1(m), from core to periphery) were obtained to reflect mineralogical zonation and to provide a spatial record through the chimney wall. Precise sample locations are shown in Fig. 3B.

From the clastic facies, samples representative of the main textural and mineralogical characteristics were obtained. These included remnant primary sulphides in addition to secondary mineral phases. Eight samples from six specimens (taken from drill cores CA-1, CA-3, CB-1, CB-2, and CB-3) were selected.

3.2. Mineralogy

Mineral identification, quantification, and textural interpretations were carried out using: (1) reflected and transmitted light microscopy; (2) electron probe microanalysis (EPMA) of selected mineral phases in the stockwork (using a Cameca SX50 based at the Natural History Museum) (Table 1); and (3) bulk chemistry, determined by ICP–AES concentration measurements of Cu, Zn, Fe, Pb, Ba and Ca in sample aliquots used for isotope measurements. It was assumed that chalcopyrite (+covellite), sphalerite, chalcopyrite+pyrite (+hematite), galena, barite, and calcite were the dominant phases present.

The stockwork specimen comprised coarsely crystalline pyrite, chalcopyrite, galena, and sphalerite, with interstitial quartz and barite, and exhibited marked mineralogical banding (Fig. 3a). The chimney sample was composed of three mineralogical zones: (1) a core of fine-grained sphalerite, surrounded by, (2) a series of concentric chalcopyrite- or sphalerite-rich overgrowths, in turn enclosed by, (3) a carapace of sphalerite with galena, pyrite, marcasite, and minor chalcopyrite (Fig. 3b). The six specimens representing the clastic facies (from drill cores CA-1, CA-3, CB-1, CB-2, and CB-3) comprise samples with high pyrite (>50%) and low sphalerite (<5%) contents, representing the upper ore horizons (CA-1 and CA-3), and samples displaying elevated (>5%) sphalerite and chalcopyrite, from the lower ore horizons and flanks (CB-1, CB-2, and CB-3). The occurrence of a fine-grained matrix of pyrite and chalcopyrite and fracture-filling bornite and covellite (Table 2) provides strong evidence for a secondary mineralization event and alteration.

Table 1
Sulphur, Mn, Fe, Co, Ni, Cu, Zn, As, Se, Ag, Cd, Sb, Te and Pb concentrations (in wt.%) for representative mineral phases of a stockwork hand specimen derived from EPMA measurements at different locations

Mineral	Location	Analysis #	S	Mn	Fe	Co	Ni	Cu	Zn	As	Se	Ag	Cd	Sb	Te
Sph	2	#71	32.50	<dt	0.06	<dt	<dt	0.07	67.29	<dt	<dt	<dt	0.54	<dt	<dt
	2	#72	32.34	<dt	<dt	<dt	<dt	<dt	66.95	<dt	<dt	<dt	0.50	<dt	<dt
	2	#73	32.36	<dt	0.08	<dt	<dt	<dt	66.75	<dt	<dt	<dt	0.57	<dt	<dt
Sph	8	#54	32.25	<dt	0.09	<dt	<dt	<dt	66.18	<dt	<dt	<dt	0.60	<dt	<dt
	8	#55	32.17	<dt	0.20	<dt	<dt	0.37	65.62	<dt	0.08	<dt	0.51	<dt	<dt
	8	#56	32.19	<dt	0.41	<dt	<dt	0.47	65.62	<dt	0.05	<dt	0.50	<dt	<dt
Ga	6	#44	13.05	<dt	0.70	<dt	<dt	0.82	<dt	<dt	0.44	0.14	<dt	0.09	<dt
	6	#45	13.36	<dt	0.76	<dt	<dt	0.90	<dt	<dt	0.42	<dt	<dt	<dt	<dt
Cpy	11	#14	34.50	<dt	30.19	<dt	<dt	33.91	1.26	<dt	<dt	<dt	<dt	<dt	<dt
	11	#15	34.27	<dt	30.09	<dt	<dt	33.47	0.68	<dt	<dt	<dt	<dt	<dt	<dt
	11	#17	34.02	<dt	29.87	<dt	<dt	33.82	0.47	<dt	<dt	<dt	<dt	<dt	0.08
Cpy	4	#27	34.27	<dt	30.84	<dt	<dt	34.31	<dt	<dt	<dt	<dt	<dt	<dt	<dt
	4	#28	34.33	<dt	30.71	<dt	<dt	34.22	<dt	<dt	<dt	<dt	<dt	<dt	<dt
	4	#29	34.08	<dt	30.71	<dt	<dt	34.25	<dt	0.08	<dt	<dt	<dt	<dt	<dt
Py	6	#39	52.70	<dt	47.19	<dt	0.06	0.26	<dt	0.10	0.08	<dt	<dt	<dt	<dt
	6	#40	52.80	0.08	47.03	<dt	<dt	0.20	<dt	0.09	<dt	<dt	<dt	<dt	<dt
	6	#41	53.18	<dt	47.15	<dt	<dt	<dt	<dt	<dt	<dt	<dt	<dt	<dt	<dt
Bn	3	#76	25.98	<dt	1.69	<dt	<dt	39.66	7.47	10.53	<dt	0.34	0.20	15.35	<dt

Sph=sphalerite (ZnS), cpy=chalcopyrite ($CuFeS_2$), py=pyrite (FeS_2), ga=galena (PbS) and bn=bornite (Cu_5FeS_4). The atomic weights (amu) used were for ZnS=97.5, for CuFeS2=183.5, Cu_5FeS_4=501.8, FeS2=119.9, and PbS=239.3. The detection limits (in ppm) were: S, 523; Mn, 572; Fe, 516; Co, 470; Ni, 525; Cu, 635; Zn, 1030; As, 704; Se, 370; Ag, 712; Cd, 901; Sb, 525; Te, 640; Bi, 693; Pb, 3242.

Table 2
δ^{65}Cu and δ^{66}Zn (in ‰), mineralogical data (in %), concentrations of Cu, Zn, Pb, Ba, Ca, and Fe (in ppm) and Cu/Zn ratios for all ore samples analysed using the MC-ICP–MS (isotopes) and ICP–AES (concentrations)

Ore facies	Sample	Mineralogy	Ba (ppm)	Ca (ppm)	Cu (ppm)	Fe (ppm)	Pb (ppm)	Zn (ppm)	Cu/Zn	δ^{66}Zn (per mill)	δ^{65}Cu (per mill)
Stockwork	SW-1(a)	cpy (100%)	531	108	307 000	350 000	10 600	24 100	12.74	−0.431	0.184
	SW-1(b)	qz (60%)+cpy (30%)+sph (10%)	8020	249	27 000	26 500	9440	194 000	0.14	0.009	0.318
	SW-1(c)	cpy (100%)	678	161	319 000	345 000	17 700	10 300	30.97	−0.418	0.163
	SW-1(d)	sph (75%)+ga (15%)+cpy (10%)		199	31 300	36 200	169 000	558 000	0.06	0.077	0.302
	SW-1(e)	cpy (85%)+sph (10%)+ga (5%)	8.6	51.9	280 000	276 000	68 100	113 000	2.48	−0.103	0.127
	SW-1(f)	ga (70%)+qz (20%)+sph (10%)	61.6	150	1030	5220	578 000	86 700	0.01	−0.031	0.277
Chimney	HV-1(a)	sph (100%)	41.8	179	15 800	18 800	11 300	598 000	0.03	−0.027	0.330
	HV-1(b)	sph (>95%)+cpy (<5%)	153	300	21 900	23 200	15 500	898 000	0.02	0.028	0.291
	HV-1(c)	sph (>95%)+cpy (<5%)	82.1	209	27 400	33 800	7560	887 000	0.03	−0.018	0.296
	HV-1(d)	cpy (80%)+sph (20%)	1380	176	285 000	301 000	9150	180 000	1.58	0.014	0.288
	HV-1(e)	sph (60%)+cpy (40%)	336	459	140 000	160 000	6750	566 000	0.25	0.030	0.281
	HV-1(f)	cpy (50%)+sph (50%)	212	137	259 000	269 000	7250	113 000	2.29	0.063	0.278
	HV-1(g)	sph (70%)+cpy (25%)+ga (5%)	181	367	93 000	102 000	49 000	618 000	0.15	0.100	0.268
	HV-1(h)	cpy (75%)+sph (25%)	168	246	274 000	307 000	6800	169 000	1.62	0.084	0.304
	HV-1(i)	sph (75%)+cpy (20%)+py (<5%)	184	173	69 400	91 700	16 200	722 000	0.10	0.121	0.279
	HV-1(j)	sph (70%)+cpy (20%)+ga (<5%)+py (<5%)	16.6	55.3	73 400	107 000	18 300	711 000	0.10	0.065	0.270
	HV-1(k)	sph (55%)+ga (20%)+cpy (15%)+py (10%)	1720	155	53 300	138 000	195 000	443 000	0.12	0.167	0.278
	HV-1(l)	sph (80%)+ga (10%)+cpy (<5%)+py (<5%)	651	166	35 300	58 500	71 600	691 000	0.05	0.231	0.294
	HV-1(m)	sph (>80%)+py (10%)+cpy (<10%)	436	374	34 600	93 700	5400	684 000	0.05	0.188	0.306
Clastic zone	CA-1	py (50%)+cpy (35%)+slc (15%)	357	1590	103 000	452 000	94	1170	88.03	–	0.054
	CA-3(b)	py (80%)+cpy (15%)+slc (5%)	277	151	40 000	445 000	297	4900	8.16	−0.295	0.278
	CB-1(a)	py (50%)+cpy (35%)+sph (10%)+slc (<5%)	224	4380	98 000	408 000	286	77 800	1.26	−0.182	0.043
	CB-1(b)	cov (<50%)+cpy (<45%)+py (<25%)+slc (15%)+sph	1370	1170	342 000	203 000	8030	76 100	4.49	−0.194	−0.300
	CB-2(a)	slc (40%)+py (30%)+cpy (20%)+sph (10%)	402	409	53 400	272 000	3360	67 900	0.79	−0.128	−0.058
	CB-2(b)	slc (60%)+py (20%)+sph (15%)+(<5%)	519	1000	20 800	167 000	6670	105 000	0.20	–	−0.009
	CB-3(a)	cpy (60%)+py (40%)	307	87.7	246 000	403 000	1740	12 200	20.16	−0.065	−0.021
	CB-3(b)	sph (65%)+py (20%)+cpy (15%)	278	85.4	76 500	182 000	866	432 000	0.18	−0.049	−0.036

δ^{65} Cu values are relative to NIST-SRM 976 Cu and δ^{66} Zn values are relative to the Lyon group JMC Zn (batch 3-0749 L). In run errors were always below 30 ppm and the over all uncertainty for the isotope data estimated using the long-term reproducibility of repeated standards was ≤0.07‰ (2σ) for both ratios. For the abbreviations of the mineral phases, see Table 1 and qz=quartz and slc=silicates. Mineralogical data are estimated from the concentration data. Samples that deviated from mass-dependent δ^{66} Zn vs. δ^{67} Zn behaviour (see text) were excluded from the table (2 out of 29).

Table 3
Ion-exchange procedure for separating Cu and Zn from geological matrices 1 prior to MC-ICP–MS isotope analysis

Elution step	Volume of elute and acid type
1	Pre-treat column with 6 ml 7 M HCl
2	Load sample in 1 ml 7 M HCl
3	Elute 6 ml 7 M HCl
4	Elute 24 ml 7 M HCl and collect the Cu fraction
5	Elute 10 ml 2 M HCl and collect the Fe fraction
6	Elute 10 ml 0.1 M HBr+0.5 M HNO_3 and collect the Zn
7	Elute 10 ml 0.5 M HNO_3 and collect the Cd fraction

This chemistry also yields >98% recoveries of Fe and Cd. Bio-Rad PolyPrep columns filled with 2.0 ml of the anion exchange resin AG MP-1 (100–200 mesh size, chloride form, Bio-Rad Laboratories, CA, USA) were used in conjunction with ultra-pure grade reagents. Columns were regenerated by back-washing with 10 ml Milli-Q H_2O before eluting 7 ml 0.5 M HNO_3 and 2 ml Milli-Q H_2O (repeated three times). The details of the ion exchange procedure is given elsewhere (Chapman et al., submitted for publication; Mason, 2003).

Mineralogical and EPMA analysis of the stockwork (Table 1) showed that sphalerite (sph) and chalcopyrite (cpy) were dominant, with levels of Cu in sphalerite and Zn in chalcopyrite normally close to or below the detection limit (e.g., locations 2 and 4, respectively). However, significant Cu was occasionally detected in sphalerite (location 8) and Zn in chalcopyrite (location 11). The bulk analyses of pure chalcopyrite separates SW-1(a) and SW-1(c) (Table 2) show that up to 1% Zn may be present in this mineral. Galena (ga) in general had small Zn concentrations, but with Cu concentrations of 600–900 ppm. Similarly, pyrite (py) was commonly enriched in Cu (up to 400–500 ppm) but with little Zn (location 6).

3.3. Reagents and standards

Acids and standards were prepared using >18.2 MΩ H_2O from a Milli-Q water system (Millipore Corporation, Bedford, MA, USA). Aristar grade reagents (VWR, Poole, UK) were used for sample preparation, and ultra-pure reagents (ROMIL Ltd., Cambridge, UK) were used during mass spectrometry. NIST-SRM 976 Cu metal was used as the reference Cu isotopic standard. No certified Zn isotopic standard is currently available, but an aliquot of the 10,000 μg/ml Zn metal solution JMC Zn, prepared from a Johnson Matthey Zn metal (batch 3-0749 L) by Maréchal et al. (1999), was used as the Zn isotopic reference standard.

3.4. Sample preparation

For sulphides free from silicate components, c. 20 mg of powdered material were digested in 5 ml 4:1 conc. HNO_3:HCl for 24 to 48 h at 100 to 120 °C in sealed Savillex PTFE vessels, before being evaporated to dryness. For samples with silicate components, c. 100 mg of powder were digested in 5:2 ml conc. HF:HNO_3 for 24 to 48 h at 100 to 120 °C in sealed Savillex PTFE vessels. Solutions were evaporated to dryness, and re-digested in 2 ml conc. HNO_3 for 24 h at 100 to 120 °C, before being evaporated to dryness again. All evaporated digests were subsequently dissolved in 2 ml 7 M HCl and volumetrically split with half being used for multi-element ICP–AES analysis, and half being used for isotope analysis.

Table 4
Operating conditions and collector configurations used in the Axiom during the study

Instrument parameters	
Coolant Ar flow	15 ml/min.
Auxiliary Ar flow	1.2–1.7 l/min.
Nebuliser Ar flow	0.75–0.95 l/min.
Ion energy	4950 V
Torch power	1250 W forward (<10 W reflected)
Cones	Pt tipped Ni sample and Ni skimmer
Nebuliser type and parameters	
Nebuliser type	Micro-concentric
Spray chamber type	Cyclonic+impact-bead set-up
Spray chamber temperature	10 °C
Sample uptake rate	c. 400 μl/min
Sensitivity	c. 40 V/ppm Cu; c. 18 V/ppm Zn
Collector (Faraday)	
Mass and position	62 (L4) – 63 (L2) – 64(L1) – 65(Ax) – 66(H1) – 67(H2) – 67.5(H3) – 68(H4)
Mass resolution	variable from $M/\Delta M$=400 to 10,000 (set to 400 for ratio)

For more details, see text.

Matrix components were separated from Cu and Zn prior to isotope analysis using anion exchange chromatography. Table 3 shows the different elution steps and the acids used. This procedure represents an amalgamation of two published methods (Maréchal et al., 1999; Strelow, 1978) and yields >98% recoveries of Cu and Zn, circumventing possible problems related to isotopic fractionation of Cu and Zn on the columns (Maréchal et al., 1999; Zhu et al., 2002). Full details of the methodology are given elsewhere (Chapman et al., submitted for publication; Mason, 2003).

Total procedural blanks for Cu and Zn were 10.9 ± 8.2 ng (2σ) and 104 ± 41 ng (2σ), respectively, based on four repeats. These represent <0.02% and <0.30% of the amount of Cu and Zn analysed for all samples. Isotopic measurements on the procedural Cu and Zn blank fractions yielded δ^{65}Cu and δ^{66}Zn values of 26.6 ± 1.2‰ (2σ) and -0.08 ± 0.05‰ (2σ), respectively, relative to NIST-SRM 976 Cu and JMC Zn. Calculations show that both the Cu and Zn procedural blank contributions have no significant influence on the final sample data within the analytical reproducibility achieved.

4. Mass spectrometry

Isotopic measurements were made using a VG *Axiom* MC-ICP-MS (Thermo Elemental, Cheshire, UK) at the NERC Isotope Geosciences Laboratory (NIGL), Keyworth, UK.

4.1. Instrumental settings

Samples were introduced to the ICP-source in solution using a Meinhard micro-concentric nebuliser with twin cyclonic/impact-bead spray chambers maintained at 10 °C. All stable isotopes of Cu and Zn, with the exception of ^{70}Zn, were measured on Faraday collectors using a static collection protocol at a spectral resolution of $M/\Delta M = 400$. Low 4 and High 3 Faraday collectors were used to monitor $^{62}Ni^{+}$ plus $^{46}Ti^{16}O^{+}$ and $^{135}Ba^{2+}$ contributions at masses 62 and 67.5, respectively. Table 4 shows the instrument settings used.

Sample and standard analyses comprised 100, 5-sec integrations, requiring 0.8 μg Cu and 2 μg Zn per analysis. Instrumental and acid-matrix related interference contributions were corrected using an acid blank on-peak baseline subtraction, and Zn hydride adducts were corrected following Mason et al. (2004a). Mass

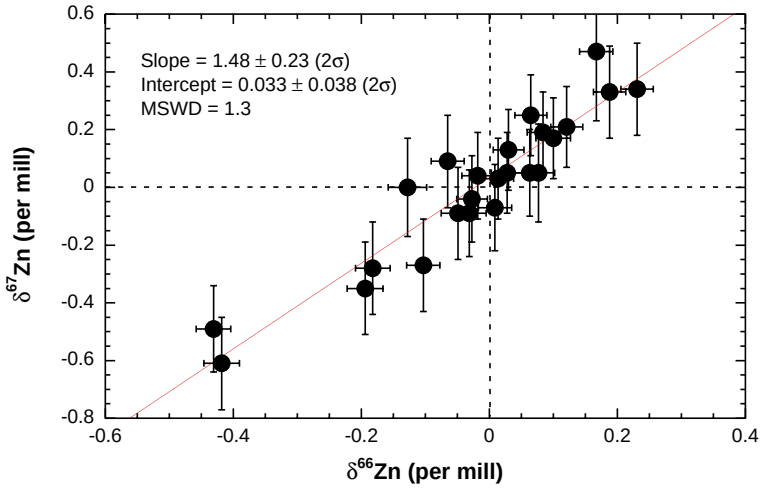

Fig. 4. δ^{66}Zn versus δ^{67}Zn for all samples discussed during the study. All δ-values are given relative to the Lyon group JMC Zn (batch 3-0749 L). Weighted regressions have been fitted to the remaining data set using IsoPlot software (Ludwig, 1982). Gradient and intercept estimates for the regression line are consistent with mass-dependent isotopic variability of Zn, indicating spectral interferences were minimal during data collection for the majority of the samples analysed. Error bars represent the $\pm 2\sigma$ combined internal precision associated with sample and standard analysed for each individual analysis.

discrimination effects were corrected using the empirical external normalisation (EEN) procedure, whereby NIST-SRM 976 Cu and JMC Zn were used as internal mass discrimination monitors, during Zn and Cu isotope measurements, respectively (Mason et al., 2004b).

4.2. Potential interferences and their correction

To assess potential isobaric interferences, all Cu and Zn column separates were analysed by ICP–AES to identify problematic contaminants that were not fully eliminated during the sample preparation procedure. For the majority of processed samples, Cu and Zn dominated the elemental budgets, with minor amounts (<5%) of K, Ca, Na, and Mg together with Fe in some Zn fractions. Potassium, calcium, and iron do not form major spectral interferences in the Cu–Zn mass range. Although measurements indicated the production of $NaAr^+$ and $MgAr^+$, the concentrations of these species were insignificant relative to the analytical reproducibility achieved. No significant Ni^+ or TiO^+ interferences were observed during data collection. Ba^{2+} interferences were corrected using an offline subtraction assuming natural abundances (Rosman and Taylor, 1998) and exponential law mass bias behaviour. The relative contribution of Ba^{2+} was always well below 1% in all the samples analysed. To assess the quality of the interference correction and the column chemistry for Zn, we analyzed all $\delta^{66}Zn$ and $\delta^{67}Zn$ data using a three-isotope plot (Fig. 4). After rejecting two out of 29 data points, the data define a significant regression with a gradient very close to the theoretical gradient of 1.48, and an intercept of within error of zero, supporting mass-dependent behavior.

4.3. Measurement reproducibility and accuracy

Reproducibility of the isotope ratio measurements was estimated by using repeated measurements of commercial metal standards, following the approach

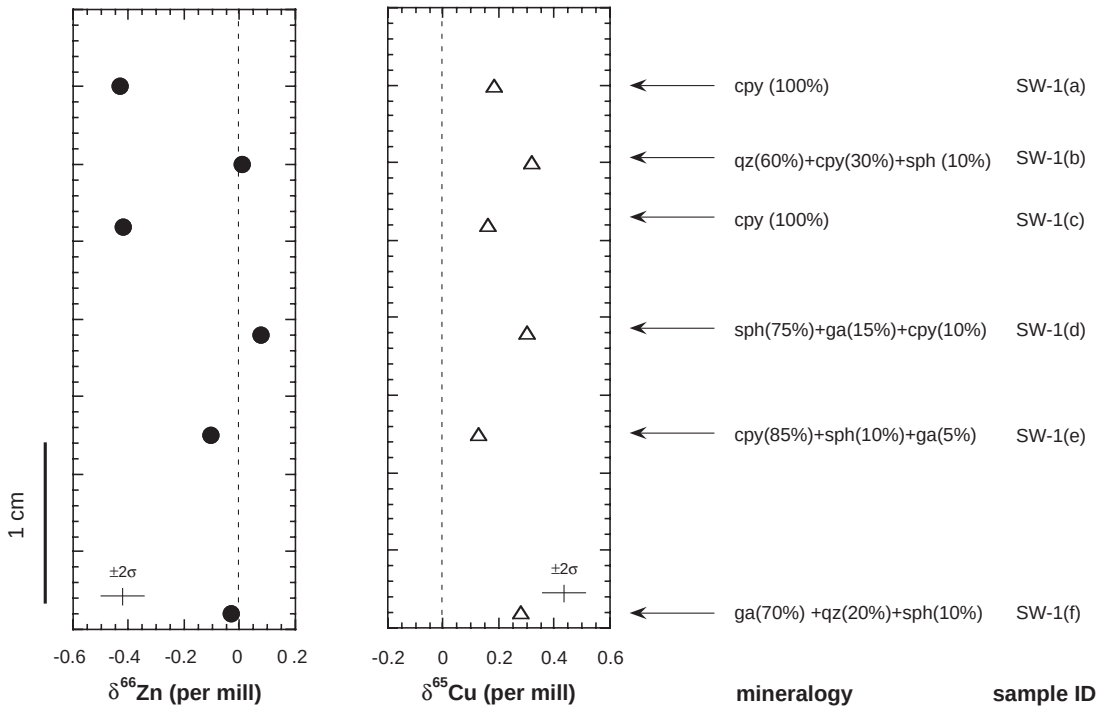

Fig. 5. Variation in $\delta^{65}Cu$ and $\delta^{66}Zn$ within the stockwork facies (SW-1). Error bars present the $\pm 2\sigma$ long-term measurement reproducibility of isotope measurements. All $\delta^{65}Cu$ and $\delta^{66}Zn$ values are relative to the NIST-SRM 976 Cu and Lyon group JMC Zn (batch 3-0749 L), respectively.

of other groups (Maréchal et al., 1999; Zhu et al., 2000). For Cu, 21 repeat analyses of the isotopic difference between NIST-SRM 976 Cu and an in-house standard, made over a 9-month period, yielded a long-term reproducibility for δ^{65}Cu of ± 0.058‰ (2σ). For Zn, the reproducibility of δ^{66} Zn measurements based on 10 repeat analyses of the isotopic difference between JMC Zn and IMP Zn over a 2-week period was ± 0.07‰ (2σ).

The accuracy of the isotope measurements was assessed measuring selected metal standards using the GVi *IsoProbe* MC-ICP-MS (GV Instruments, Manchester, UK), based in the Natural History Museum/Imperial College London Joint (NHM-ICL JAF) Analytical Facility, using sample-standard bracketing following a previously outlined protocol (Mason et al., 2004b). The relative isotopic compositions of the Cu and Zn metal standards are in good agreement between the two instruments, being within error in all cases. Furthermore, the value for JMC Cu are within uncertainty to those reported by the Lyon group (Maréchal et al., 1999). No memory effects were noticed.

5. Isotopic variability of Cu and Zn at Alexandrinka

Copper and Zn in ore samples from the Alexandrinka deposit show a range in δ^{65}Cu and δ^{66}Zn values of -0.30 to 0.32‰ and -0.43 to 0.23‰, respectively (Table 2). These deviations are significant compared to the analytical uncertainties associated with the long-term reproducibility. The restricted range in δ^{65}Cu at Alexandrinka, including results from the supergene assemblage in the lower horizons of the deposits, is unlike modern sulphides at mid oceanic ridges where a large range of δ^{65}Cu, of up to 3‰, is observed (Rouxel et al., 2004; Zhu et al., 2000).

5.1. Isotopic variability in the stockwork

For Zn, significant isotopic variations are observed in the stockwork samples (Fig. 5), with samples containing pure chalcopyrite (SW-1(a) and SW-1(c)) being depleted in isotopically heavy Zn by c. 0.2‰ pamu relative to samples containing sphalerite, such as

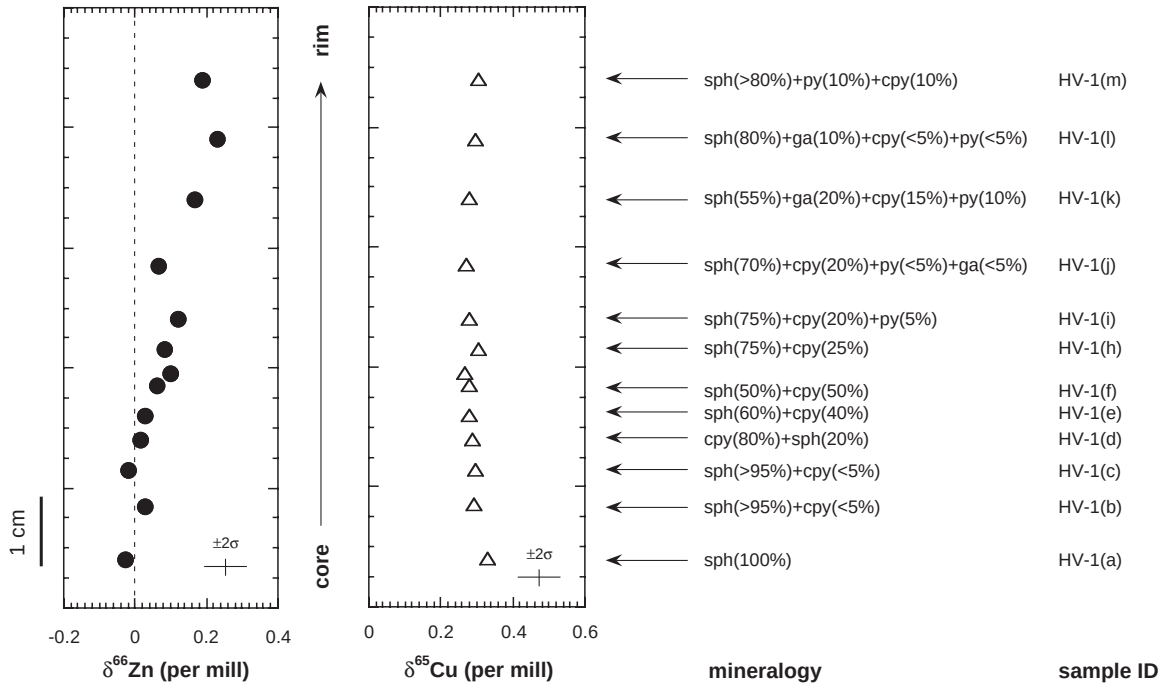

Fig. 6. Variation in δ^{65}Cu and δ^{66}Zn from core (HV-1(A)) to periphery (HV-1(m)) through the hydrothermal chimney (HV-1). Error bars present the $\pm 2\sigma$ long-term measurement reproducibility of isotope measurements. All δ^{65}Cu and δ^{66}Zn values are relative to the NIST-SRM 976 Cu and JMC Zn (batch 3-0749 L) standards, respectively.

SW-1(b), SW-1(d), SW-1(e), and SW-1(f). Similarly for Cu, samples dominated by chalcopyrite (SW-1(a), SW-1(c), and SW-1(e)) are depleted in isotopically heavy Cu by c. 0.07‰ pamu relative to samples dominated by quartz (SW-1(b)), sphalerite (SW-1(d)), and galena (SW-1(f)) The ranges measured for both δ^{65}Cu and δ^{66}Zn are in good agreement with published data from other primary Cu and Zn mineralization (Graham et al., 2004; Larson et al., 2003; Rouxel et al., 2004; Wilkinson et al., in press).

5.2. Isotopic variability in the chimney

Copper and Zn isotope data from the core to the periphery of the hydrothermal chimney (HV-1) are presented in Fig. 6. δ^{65}Cu is invariant within error of the measurements throughout the chimney wall, and the average δ^{65}Cu value for the vent material of 0.29 ± 0.03‰ (2σ) is within error of the average composition of the stockwork at 0.23 ± 0.16‰ (2σ) (Fig. 5). The pattern suggests that Cu isotopes are not significantly fractionated during chimney formation. In contrast, for Zn, whilst the core yields a similar composition to the sphalerite-rich stockwork (Table 2), a systematic increase in δ^{66}Zn away from the core is observed, with the periphery being enriched by up to 0.23‰. This shift is over three times greater than the analytical uncertainty on the measurements. Unlike the stockwork, no clear correlation exists between δ^{66}Zn and mineralogy. All

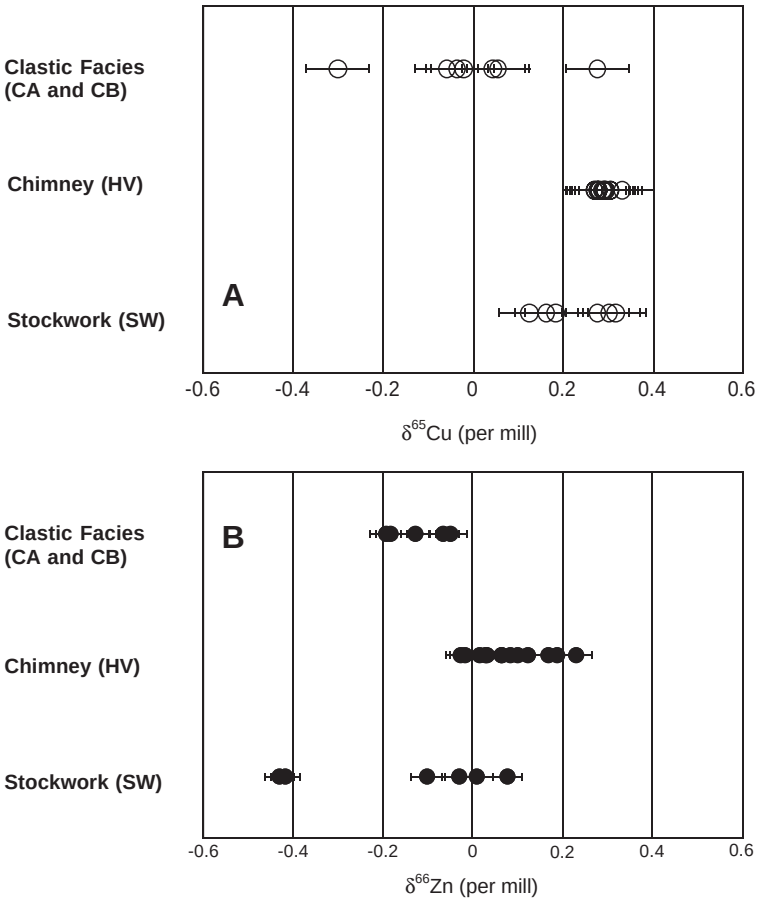

Fig. 7. Variation in (A) δ^{65}Cu and (B) δ^{66}Zn in the clastic sediments. All Cu and Zn isotope data are given relative to NIST-SRM 976 Cu and the Lyon group JMC Zn (batch 3-0749 L) standard, respectively. Analytical errors associated with the measurements are ± 0.07‰ ($\pm 2\sigma$) for both δ^{65}Cu and δ^{66}Zn.

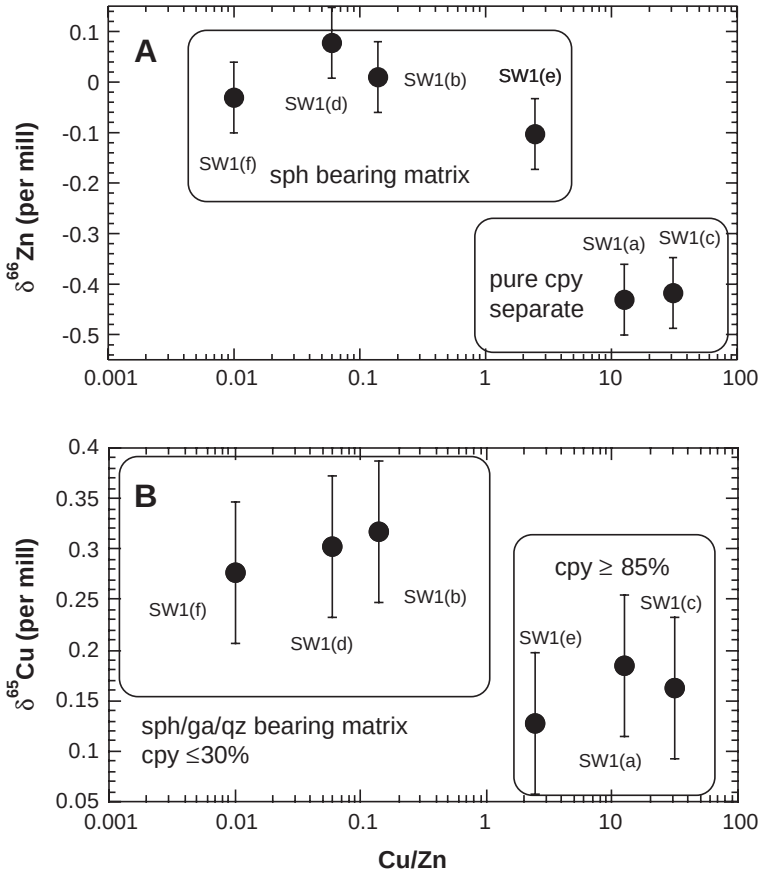

Fig. 8. δ^{66}Zn vs. Cu/Zn (A) and δ^{65}Cu vs. Cu/Zn (B) in the stockwork samples. There is an apparent control of the isotopic compositions of Zn and Cu via the mineralogy and thus the Cu/Zn ratio. See text for details.

samples contain >20% sphalerite, which therefore dominates the Zn budget of all of the chimney samples analysed.

5.3. Isotopic variability in the clastic facies

For the clastic ore facies the range in δ^{65}Cu, from −0.30 to 0.28‰, is five times greater than the range observed for the stockwork and hydrothermal vent samples (Fig. 7 and Table 2). These results partially fall within the range observed in the chimney (0.33 to 0.27‰) and stockwork (0.18 to 0.32‰) samples, but extend to significantly lower δ^{65}Cu values.

The δ^{66}Zn values for samples from the clastic facies vary between −0.05 and −0.295‰. Again, this range partially overlaps with stockwork and chimney sample data, and also spread toward lower values than the chimney sample (Fig. 7).

6. Mechanisms of isotopic fractionation

6.1. Mineralogical fractionation in the stockwork

The isotopic compositions of Zn and Cu within the stockwork samples are dependent on the mineralogy (Table 2; Figs. 6 and 8). The two pure chalcopyrite separates (SW-1(a) and SW-1(c)) that have high Cu/Zn ratios are enriched in light Zn isotopes (δ^{66}Zn of −0.431 and −0.418‰) compared to those samples that contain significant sphalerite (e.g. SW-1(b), SW-1(d), SW-1(e), and SW-1(f)). Substitution of Zn for Cu can occur in

chalcopyrite (Deer et al., 1992), and this is confirmed by the high Zn concentrations measured in the two chalcopyrite separates. The occurrence of microscopic inclusions of sphalerite in these samples can be excluded based on reflected light and scanning electron microscopy.

The observed difference in δ^{66}Zn between coexisting chalcopyrite and sphalerite is considered to be most likely due to equilibrium isotopic fractionation of Zn between the two minerals during their formation. Sulphur isotope data from coexisting sulphides within the stockwork support equilibrium formation conditions at around 300 °C (Tessalina et al., 1999). The same mechanism has been suggested for copper isotope fractionation between coexisting chalcopyrite and bornite from high-temperature mineral deposits (Larson et al., 2003).

The copper isotope data also appear to suggest a mineralogical control. Three of the samples with high chalcopyrite content (SW-1(a), SW-1(c), and SW-1(e)) have δ^{65}Cu values below 0.2‰ (Table 2, Fig. 8) whereas samples with higher concentrations of other phases such as sphalerite and galena (SW-1(f), SW-1(d)) have δ^{65}Cu values above 0.2‰. EPMA data confirm that considerable concentrations of Cu are found locally in sphalerite (location 8, Table 1) and galena (location 6, Table 1). The more pronounced homogeneity in the Cu isotope composition of chalcopyrite in the stockwork samples suggests that Cu isotopes are less strongly fractionated during relatively high-temperature hydrothermal precipitation and that the stockwork zone is protected from later low-temperature modification that could affect samples from closer to the seawater interface (e.g. Zhu et al., 2000; Rouxel et al., 2004). Post-depositional homogenisation due to recrystallisation at very low metamorphic grades is not likely.

6.2. Zn isotope variation during sphalerite precipitation in the chimney

In the chimney samples, δ^{66}Zn systematically increases from core to rim (Fig. 6). The similarity in δ^{66}Zn values between the inner chimney wall and sphalerite from the stockwork (both of which formed at c. 300 °C from presumably similar fluid compositions) and the spatial distribution through the chimney wall, suggest a syngenetic origin for the zinc isotope variation. This is possibly due to temperature-controlled variations in the sphalerite–aqueous zinc fractionation factor, or a localised Raleigh distillation effect during fluid transport through the porous chimney wall, similar to mechanisms proposed for Zn isotope variations in Irish Zn–Pb ores (Wilkinson et al., in press).

6.3. Secondary alteration in the clastic sediments

In the clastic facies the δ^{65}Cu and, to a lesser degree, δ^{66}Zn values are lower than those for the chimney (Fig. 7). The shift to lighter isotopic compositions for both metals is associated with the development of secondary Cu- and Zn-bearing mineral phases (Table 2), dominated by secondary sphalerite and chalcopyrite.

The occurrence in sample CB-1(b) of secondary covellite with a low δ^{65}Cu value of −0.30‰ in a matrix of py+cpy (CB-1(a)) with a δ^{65}Cu value of 0.04‰ (see Table 2 and Fig. 7) is consistent with a depletion in ^{65}Cu during secondary mineralization. Preferential incorporation of light ^{63}Cu during covellite precipitation has been demonstrated experimentally (Ehrlich et al., 2004). In addition, previous work reporting bornite–chalcopyrite mineral pairs from a variety of ore deposit types suggested an enrichment of lighter ^{63}Cu in secondary phases (Larson et al., 2003; Rouxel et al., 2004). The greater spread of δ^{65}Cu values in the clastic sulphides compared to the stockwork and chimney samples agrees with previous studies where secondary minerals have been observed to have a greater range copper isotope composition compared to the primary deposits (Larson et al., 2003; Walker et al., 1958).

The wider range in Cu isotope composition within the clastic facies, relative to the primary mineralization, is probably controlled by redox reactions during remobilization of Cu within the sediment pile. Chalcopyrite is the dominant primary Cu-bearing mineral phase within the clastic sediments, and likely represents the main source of Cu for the secondary mineralization. Copper is present within the chalcopyrite structure as Cu(I) (Greenwood and Whitfield, 1968; Nakai et al., 1978). However, during oxidative dissolution of chalcopyrite, Cu(I) is oxidized to Cu(II), with this oxidation step being controlled by the

physico-chemical conditions under which the dissolution occurs (Buckley and Woods, 1984; Hackl et al., 1995). The presence of oxidised, gossan-like horizons within the clastic sequence suggests that conditions at or near to the seafloor were strongly oxidizing, and Cu released during the decomposition of primary chalcopyrite is thus predicted to have been oxidised to Cu(II). Copper concentrations in the gossans are very low (c. 50 μg/g), indicating near-complete removal of Cu during leaching. Under such conditions the Cu(II)-bearing fluids generated would have inherited the isotopic composition of primary chalcopyrite, with a δ^{65}Cu composition of c. 0.27‰ (the average of the stockwork and chimney data). It is considered likely that as this fluid migrated down-section within the sediment pile and conditions became more reducing, redox conditions changed sufficiently for Cu(II) to be reduced back to Cu(I). This reduction accompanied precipitation of Cu(I)-bearing phases including chalcopyrite, bornite, and covellite. Experimental studies have shown that the reduction of Cu(II) to Cu(I) induces isotopic shifts of 3–4‰ towards isotopically light compositions in the Cu(I) product (Ehrlich et al., 2004; Zhu et al., 2002). Thus, the shift towards light Cu isotopic compositions with secondary mineralization within the enrichment zone may reflect reduction of Cu(II) to Cu(I) associated with this secondary mineralization event.

7. Conclusions

Isotopic variability for Cu and Zn has been observed in the Alexandrinka VHMS deposit. The data allow further constraints to be placed on the controls and extent of transition metal isotope fractionation in ore deposits and ancient seafloor hydrothermal mineralization.

The combined δ^{65}Cu and δ^{66}Zn values of all three facies define the three main mechanisms inferred to control the isotopic compositions of Cu and Zn in the Alexandrinka deposit (Fig. 9). The initial hydrothermal fluid composition has δ^{65}Cu and δ^{66} Zn values of 0.2 ± 0.15‰ and of 0.0 ± 0.1‰, respectively. This agrees well with previously suggested 'bulk Earth' (Graham et al., 2004; Larson et al., 2003; Maréchal et al., 1999; Wilkinson et al., in press).

Fractionation of copper and zinc isotopic signatures away from these initial compositions is thought

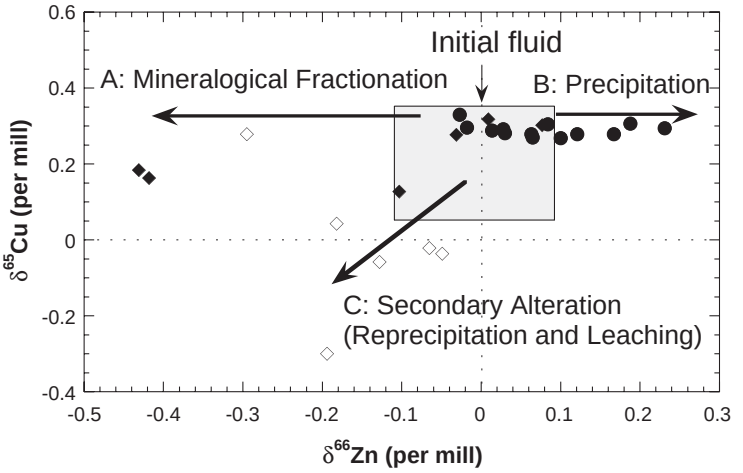

Fig. 9. A summary plot showing δ^{66}Zn vs. δ^{65}Cu of all three facies assessed within the VMHS deposit, both for primary mineralization (stockwork, ♦, and chimney, ●) and secondary mineralization and alteration products (◇). The initials fluid has a δ^{65}Cu of 0.2 ± 0.15 and δ^{66}Zn of 0.0 ± 0.1, which agrees with values suggested for 'bulk earth' by other groups (Larson et al., 2003; Wilkinson et al., in press). There are three major fractionation mechanisms which we postulate: (A) Isotopically light Zn is accommodated into the chalcopyrite structure (samples SW-1(a) and SW-1(c)). (B) Syngenetic variation in sphalerite isotopic composition enriching heavy Zn toward the periphery of the chimney. (C) Seafloor alteration (mainly due to re-mineralisation and leaching) leads to isotopic lighter Cu and Zn signatures in the clastic sediments – characterised by secondary Cu and Zn minerals – relative to the chimney.

to be due to three distinct processes, each forming the major control in a different portion of the deposit. Broadly these can be summarised as:

A. Equilibrium isotopic partitioning of Zn into chalcopyrite favours isotopically light Zn being accommodated into the chalcopyrite structure. This leads to significant isotopic variability for Zn in the stockwork, where light values coincide with chalcopyrite-rich areas. This effect is less clear for Cu.
B. Syngenetic Zn isotope fractionation occurs as hydrothermal fluids percolate through the porous vent wall. The mechanisms controlling this variation remain poorly constrained but we regard the two most likely explanations to be a temperature-controlled fractionation-factor variation, or local distillation fractionation exaggerating a small inherent mineralogical fractionation. This effect is not significant for Cu.
C. Re-precipitation during gossan genesis as leached fluids migrated down-section and possibly seafloor alteration involving leaching produces a shift toward lighter isotopic compositions for Cu and Zn in the clastic sediments, relative to chimney and stockwork. The variation of Cu in the clastic sediments is larger than in the chimney and stockwork. This is consistent with redox-induced isotopic fractionation during the incomplete precipitation of Cu from enriched brines within the clastic sulphide pile.

The restricted range in δ^{65}Cu at the Alexandrinka VHMS, including within the supergene assemblage in the lower horizons of the deposits, is unlike modern sulphides at mid ocean ridges where a large range of Cu isotope compositions, of up to 3‰, has been reported (Rouxel et al., 2004; Zhu et al., 2000).

Acknowledgements

We wish to thank the Natural Environmental Research Council (NERC) for ongoing support of the laboratory facilities used during the study and for funding the CASE PhD scholarship under which this work was undertaken. We are very grateful to C. P. Ingle, G. Nowell, R. McGill and V. Pashley who all contributed to the analyses on the Axiom. A. Dolgopolova, S. S. Russell, E. Mullane, M. Gounelle, T. Jeffries, V. Din, G. Jones, and T. Williams are thanked for their help in running the laboratories at the Natural History Museum where the sample preparation was undertaken. We also thank R. Herrington from the Natural History Museum for access to the ore samples and Randall R. Parrish for access to the analytical facilities at NIGL. We thank B. Beard, J. Ripley and two anonymous reviewers for helpful comments on an earlier version of the paper and R. Rudnick for editorial handling. Finally we wish to acknowledge A. Fleet, M. Warner and the Leverhulme Trust for helping finance this work. **[RR]**

References

Archer, C., Vance, D., 2002. Isotopic fractionation of Fe, Cu and Zn associated with Archean microbially mediated sulphides. Geochim. Cosmochim. Acta 66 (15A), A26.

Belogub, E.V., Novoselov, C.A., Spiro, B., Yakovleva, B.A., 2003. Mineralogical and S isotopic features of the supergene profile of the Zapadno–Ozernoe massive sulphide and Au bearing gossan deposit, South Urals. Mineral. Mag. 67 (2), 339–354.

Blix, R., Ubisch, H.V., Wickman, F.E., 1957. A search for variations in the relative abundance of the zinc isotopes in nature. Geochim. Cosmochim. Acta 11 (3), 162–164.

Buckley, A.N., Woods, R., 1984. An X-ray photoelectron spectroscopy study of the oxidation of chalcopyrite. Aust. J. Chem. 37, 2403–2413.

Chapman, J., Mason, T.F.D., Weiss, D.J., Coles, B.J., Wilkinson, J.J., submitted for publication. Chemical separation and isotopic variations of Cu and Zn from five geological reference material. Geostand. Geoanal. Res.

Deer, W.A., Howie, R.A., Zussman, J., 1992. An introduction to the rock-forming minerals. Longman Scientific and Technical.

Ehrlich, S., Butler, I., Halicz, L., Rickard, D., Oldroyd, A., Matthews, A., 2004. Experimental study of copper isotope fractionation between aqueous Cu(I) and covellite, CuS. Chem. Geol. 209, 259–269.

Gale, N.H., Woodhead, A.P., Stos-Gale, Z.A., Walder, A., Bowen, I., 1999. Natural variations detected in the isotopic composition of copper: possible applications to archaeology and geochemistry. Int. J. Mass Spectrom. 184, 1–9.

Graham, S., Pearson, N., Jackson, S., Griffin, W., Reilly, S.Y.O., 2004. Tracing Cu and Fe from source to porphyry: in situ determination of Cu and Fe isotope ratios in sulfides from the Grasberg Cu–Au deposit. Chem. Geol. 207, 147–169.

Greenwood, N.N., Whitfield, H.J., 1968. Mössbauer effect studies on cubanite ($CuFe_2S_3$) and related iron sulphides. J. Chem. Soc. A., Lond. 7, 1697–1699.

Hackl, R.P., Dreisinger, D.B., Peters, E., King, J.A., 1995. Passivation of chalcopyrite during oxidative leaching in sulfate media. Hydrometallurgy 39 (1), 25–48.

Herrington, R.J., et al., 2002. Massive sulfide deposits in the South Urals: geological setting within the framework of the Uralide orogen. Mountain Building in the Uralides: Pangaea to the Present. American Geophysical Union, pp. 155–182.

Jiang, S., Woodhead, J., Yu, J., Pan, J., Liao, Q., Wu, N., 2002. A reconnaissance of Cu isotopic compositions of hydrothermal vein-type copper deposit, Jinman, Yunnan, China. Chin. Sci. Bull. 47 (3), 247–250.

Johnson, C.M., Beard, B.L., Albarède, F., 2004. Geochemistry of non-traditional stable isotopes. Reviews in Mineralogy and Geochemistry, vol. 55. Mineralogical Society of America. 453 pp.

Larson, P.B., et al., 2003. Copper isotope ratios in magmatic and hydrothermal ore-forming environments. Chem. Geol. 201, 337–350.

Ludwig, K., 1982. A Computer Program to Convert Raw U–Th–Pb Isotope Ratios to Blank-Corrected Isotope Ratios and Concentrations With Associated Error Calculation. OF.-88-0557. U.S. Geological Survey.

Maréchal, C.N., Télouk, P., Albarède, F., 1999. Precise analysis of copper and zinc isotopic compositions by plasma-source mass spectrometry. Chem. Geol. 156, 251–273.

Mason, T.F.D., 2003. High precision transition metal isotope analysis by plasma-source mass spectrometry and implications for low temperature geochemistry. PhD thesis, Imperial College, London, 287 pp.

Mason, T.F.D., Weiss, D.J., Horstwood, M., Parrish, R.R., Russell, S.S, Mullane, E., et al., 2004a. High precision Cu and Zn isotope analysis by plasma source mass spectrometry: Part 1. Spectral interferences and their correction. J. Anal. At. Spectrom. 19 (2), 209–217.

Mason, T.F.D., Weiss, D.J., Horstwood, M., Parrish, R.R., Russell, S.S, Mullane, E., et al., 2004b. High precision Cu and Zn isotope analysis by plasma source mass spectrometry: Part 2. Correcting for mass bias discrimination effects. J. Anal. At. Spectrom. 19 (2), 218–226.

Nakai, I., Sugitani, Y., Nagashima, K., 1978. X-ray photoelectron spectroscopic study of copper minerals. J. Inorg. Nucl. Chem. 40, 781–791.

Prokin, V.A., Buslaev, F.P., Nasedkin, A.P., 1998. Types of massive sulfide deposits in the Urals. Miner. Depos. 34 (10), 121–126.

Rosman, K.J.R., Taylor, P.D.P., 1998. Isotopic compositions of the elements 1997. J. Anal. At. Spectrom. 13 (10), 45–55.

Rouxel, O., Fouquet, Y., Ludden, J.N., 2004. Copper isotope systematics of the Lucky Strike, Rainbow, and Logatchev sea-floor hydrothermal fields on the Mid-Atlantic Ridge. Econ. Geol. 99, 585–600.

Scott, S.D., 1981. Small chimneys from Japanese Kuroko deposits. In: Goldie, R., Botrill, T.J. (Eds.), Seminars on Seafloor Hydrothermal Systems. Geoscience Canada, pp. 103–104.

Shanks, W., Seyfried, W., 1987. Stable isotope studies of vent fluids and chimney minerals, southern Juan de Fuga Ridge: sodium metasomatism and seawater sulphate reduction. J. Geophys. Res. 92, 11387–11399.

Shields, W.R., Goldich, S.S., Garner, E.L., Murphy, T.J., 1965. Natural variations in the abundance ratio and the atomic weight of copper. J. Geophys. Res. 70 (2), 479–491.

Sigov, A., 1969. Mesozoic and Cenozoic ore formation in the Urals. Nedra, Moscow.

Strelow, F.W.E., 1978. Distribution coefficients and anion exchange behaviour of some elements in hydrobromic–nitric acid mixtures. Anal. Chem. 50, 1359–1361.

Tessalina, S.G., Maslennikov, V.V., Zaykov, V.V., Orgeval, J.J., 1999. Ore facies of the Alexandrinka massive sulphide deposit, South Urals. In: Stanley, C. (Ed.), Mineral Deposits: Processes to Processing. Balkema, pp. 601–604.

Tessalina, S.G., Zaykov, V.V., Orgeval, J.J., Auge, T., Omeneto, B., 2001. Mafic–ultramafic hosted massive sulphide deposits in southern Urals (Russia). Mineral Deposits at the Beginning of the 21st Century. Balkema, Rotterdam, pp. 353–356.

Walker, E.C., Cuttitta, F., Senftle, F.E., 1958. Some natural variations in the relative abundances of copper isotopes. Geochim. Cosmochim. Acta 15, 183–194.

Weiss, D.J., Mason, T.F.D., Zhao, F.J., Kirk, G.J.D, Coles, B.J., Horstwood, M.S.A., 2005. Isotopic discrimination of Zn in higher plants. New Phytol. 165, 703–710.

Wilkinson, J.J., Weiss, D.J., Coles, B.J., Mason, T.F.D., in press. Controls of zinc isotope variability in ore-forming systems: preliminary constrains from the Zn–Pb Irish ore fields. Econ. Geol.

Zhu, X.K., O'Nions, R.K., Guo, Y., Belshaw, N.S., Rickard, D., 2000. Determination of natural Cu-isotope variation by plasma source mass spectrometry: implications for use as geochemical tracers. Chem. Geol. 163, 139–149.

Zhu, X.K., Guo, Y., Williams, R.J.P., O'Nions, R.K., Matthews, A., Belshaw, N.S., et al., 2002. Mass fractionation processes of transition metal isotopes. Earth Planet. Sci. Lett. 200, 47–62.